

An alternative method for measuring total respiratory resistance during quiet breathing: a feasibility and validation study

N. ANAGNOSTOPOULOS¹, A. TZORTZI², K. CHOLIDOU¹,
V. EVANGELOPOULOU², G. KALTSAKAS^{3,4}, E. KOUKAKI¹,
G. STRATAKOS¹, M. LYMPERI⁵, P. BEHRAKIS², M. KOUTSILIERIS⁵

¹First Respiratory Clinic, Medical School, National and Kapodistrian University of Athens, Sotiria Hospital, Athens, Greece

²George D. Behrakis Research Lab, Hellenic Cancer Society, Athens, Greece

³Lane Fox Respiratory Service, Guy's and St Thomas' NHS Foundation Trust, London, UK

⁴Centre of Human and Applied Physiological Sciences, Faculty of Life Sciences and Medicine, King's College, London, UK

⁵Department of Physiology, Medical School, National and Kapodistrian University of Athens, Greece

Abstract. – OBJECTIVE: Determining the respiratory system's mechanical properties with minimal patient effort has been an important field of investigation addressing patients unable to perform pulmonary function testing and in light of the preventive measures due to the recent pandemic. The current study aimed to present an alternative method for total respiratory resistance measurement during tidal breathing, compare it with airway resistance (R_{aw}), measured by body plethysmography, and validate the procedure in three groups of subjects with normal, constrictive and obstructive respiratory patterns in spirometry.

PATIENTS AND METHODS: We developed an alternative method of assessing total respiratory resistance during quiet breathing. After manufacturing the appropriate hardware apparatus, we applied a steady extrinsic resistance (ΔR) for 100-200 m/s during tidal breathing. A theoretical mathematical model allowed measurement of total respiratory resistance (R_{tot}) during inspiration (R_{in}) and expiration (R_{ex}). To validate the method, 15 individuals were enrolled and assigned to the normal, obstructive and restrictive groups based on their spirometry patterns. All groups participated in two sets of measurements, the plethysmographic and novel method. Finally, respiratory resistance measurements were compared between groups and methods.

RESULTS: The method was successfully developed, and R_{tot} measurements were recorded in five normal subjects and in five obstructive and restrictive subjects. Mean R_{in} and

mean R_{ex} were 4.99 cm H₂O/L/sec and 4.42 cm H₂O/L/sec in the healthy, 4.87 cm H₂O/L/sec, and 6.63 cm H₂O/L/sec in the obstructive and 5.97 cm H₂O/L/sec and 4.12 cm H₂O/L/sec in the restrictive group, respectively. R_{ex} was notably higher than R_{in} in the obstructive group and was positively correlated with R_{aw} ($p < 0.005$, $r = 0.47$).

CONCLUSIONS: This method provides the theoretical background for a plausible alternative tool for accessing a mechanical parameter of the respiratory system, which is easy to perform and requires only passive patient cooperation while enabling rough differentiation between obstructive and restrictive disorders. The model's feasibility potential in a real-life setting was studied in a small sample, and additional implementation and validation of the method in a larger population are guaranteed.

Key Words:

Lung mechanics, Mathematical models, Respiratory resistance, Lung function tests, Tidal breathing, Inspiratory phase, Expiratory phase.

Introduction

Pulmonary function tests (PFTs) are invaluable in disease diagnosis, severity grading, and treatment response. Although spirometry is readily available and performed routinely, being a forced manoeuvre, its results suffer significant

variability, often depending on patient cooperation^{1,2}. Furthermore, children, elderly patients, and patients with end-stage disease, neuromuscular disorders or cognitive impedance are usually unable to perform PFTs. In light of the Sars-COV2 pandemic, lung function laboratories have implemented strict pre-procedure standards and preventive measures to limit the spread. This led to a significant decrease in patients undergoing lung function evaluation.

Measuring the mechanical properties of the respiratory system during quiet breathing, including total respiratory resistance (R_{tot}), has been proposed as an alternative in the above populations and can be helpful. Various effortless modalities exist, the most popular being the body plethysmography, the complete occlusion technique (Roc) and the impulse oscillometry system (IOS).

Currently, insight into respiratory resistance in everyday clinical practice is provided by the body plethysmography method³. However, it reflects only airway resistance (R_{aw}) and requires specific respiratory maneuvers performed by the patient. The shutter technique for measuring Roc is based on a total occlusion of the patient's expiratory flow⁴. Despite being effortless, recognizing the occlusion from the patient may alter the neuromuscular status and, therefore, temper the results. Moreover, Roc fails to differentiate various pathologies and has not been used for partitioning inspiratory and expiratory resistance.

The most often applied test that can measure airway resistance and reactance, requiring only passive patient cooperation, is the impulse oscillometry technique (IOS)^{5,6}. This method's main drawback is the lack of standardized normal values and specificity and the inability to accurately differentiate between the major types of functional respiratory impairment.

To the authors' knowledge, there is currently a scarcity of methods that examine lung function and particularly respiratory mechanics under conditions of resting breathing, a rising necessity in light of the recent pandemic.

Therefore, the current study aimed to develop a novel model to measure total respiratory resistance during quiet breathing and describe the model's theoretical background and mathematical equations. Furthermore, the study aimed to examine the potential to differentiate between obstructive and restrictive respiratory impairment and validate the procedure.

Patients and Methods

Theoretical Background and Mathematical Model

Respiratory System's Equation of Motion

The respiratory system can be represented with several theoretical analogues (physical, electrical, mathematical) of variable complexity according to the number of compartments of each model and their relative positioning (i.e., parallel or in series)⁷. Each compartment substitutes an anatomical or, most frequently, a physiological unit of the respiratory system, such as the alveolar space, the airways or the chest wall. A set of dependent (pressure, volume, flow, acceleration of flow) and non-dependent variables (compliance, resistance) can be applied to each of these parts to describe the model's viscoelastic properties under various conditions⁸.

The respiratory system's equation of motion relates its pressure conduct to the different volume and airflow values and its mechanical characteristics (elastance and resistance).

During quiet inspiration in a non-ventilated subject, the driving pressure (P_{drive}) equals the pressure difference across the entire respiratory system and is mainly generated by the diaphragm (P_{mus}).

$$P_{drive} = P_{atm} - P_{mus} \quad \text{Eq. (1)*,}$$

where $P_{atm} = 0$

This pressure increment must overcome the opposing pressures generated by the system's moving parts' tendency to return to their equilibrium point once deformed by a spatial quantity (i.e. volume in the case of the respiratory system). This elastic behaviour can be studied both from a static and dynamic perspective, although instantaneously when airflow is 0, the static recoil pressure (P_{sr}) can be easily assessed.

All the moving parts of the respiratory system resist motion. Thus, the input energy (force of muscles) and the dynamic energy stored in the tissues (elasticity) dissipate and are released as heat due to resistance. Pressures generated due to resistance

*: In this equation, the transabdominal and rib cage compartments connected in parallel to the system are considered negligible.

(Pres) are always dynamic, mainly attributed to the column of moving air through the airways and the deformation of the tissue parenchyma.

Finally, the moving parts' resistance to direction changes, and their ability to store kinetic energy is called inertia. It produces pressures (Pin) that correlate with the flow's acceleration and the mass of the moving parts, but they can be negligible in the setting of low frequencies such as tidal breathing. Combining the above,

$$P_{drive} = P_{sr} + P_{res} + P_{in} \quad \text{Eq. (2)}$$

The respiratory system's equation can be written as:

$$-P_{mus} = V(t)E + V'(t)R + V''(t)I + P_0 \quad \text{Eq. (3)}$$

$V''(t)$ is the flow acceleration, and P_0 is positive end-expiratory pressure (usually added during mechanical ventilation and generally considered zero unless there is severe hyperinflation, i.e. emphysema). The term I is the coefficient of flow acceleration.

During passive expiration, P_{drive} equals the elastic recoil pressure of the lungs and tissue parenchyma (P_{el}) and needs only to overcome the resistive elements of the system (P_{res}), thus

$$P_{drive} = P_{el} = V'(t)R + V''(t)I \quad \text{Eq. (4)}$$

Single Compartment Model of the Respiratory system

Our study is based on the viscoelastic single-compartment model proposed by Bates et al¹⁰ in 1985. The respiratory system can be depicted as a single airway connected to an expandable elastic chamber in this model. The addition of mechanical properties of the tissues (Known as a Maxwell body) can be seen in Figure 1⁹. When a ramp-pressure is applied, the equation describing it during inspiration is:

$$V(t)E + V'(t)R = at \quad \text{Eq. (5)}$$

Where $V(t)$ is volume, $V'(t)$ it's time derivative (flow), E is Elastance (the reciprocal of compliance), and R is Resistance. And

$$V(t) = (\alpha\tau/E) e^{-t/\tau} + \alpha t/E - \alpha\tau/E \quad \text{Eq. (6)}$$

Where a is the slope of the pressure-volume curve, and $\tau = R/E$ is the time constant of the system.

This is very close to the description of quiet breathing, especially mid-quiet inspiration, where the flow is steady, the resistance is close to linear, and the exponential term of Eq. (2) fades away. Since P_{drive} is proportional to time ($P_{drive} = at$), Eq. (5) can be rewritten as

$$P(t) = V(t)E + P_{res} \quad \text{Eq. (7)}$$

Also, in mid-inspiration with a steady (or near steady) flow and the resistance reaching constant values:

$$P_{drive} = V(t)E + V'(t)R \quad \text{Eq. (8)}$$

This is the same equation of motion (Eq. 3) if we neglect the inertive element ($V''(t)I$) and $P_0 = 0$.

A Mathematical Model for Measuring Total Resistance

To evaluate total respiratory resistance in the current study, we measured respiratory flow changes by applying an extrinsic resistance during tidal breathing. A rapid, instantaneous flow decrease is observed when a standard external resistance is applied during inspiration or expiration. This enables the application of the equation of motion at two specific time points; the first right before the implementation of the exogenous resistance and the second during its application when the peak mouth pressure (P_{mouth}) is observed. Given that the flow decrease is rapid (100-200 m/s), the neuromuscular system cannot identify the extrinsic "obstacle" and does

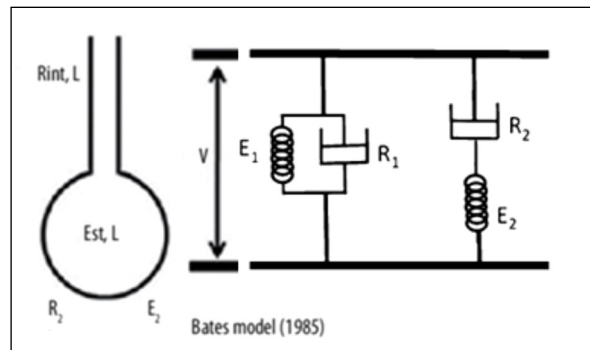


Figure 1. Bates model. The single compartment linear model consists of a single pulmonary pathway and the addition of a Maxwell body (R_2, E_2) (airway and bicompartamental viscoelastic unit).

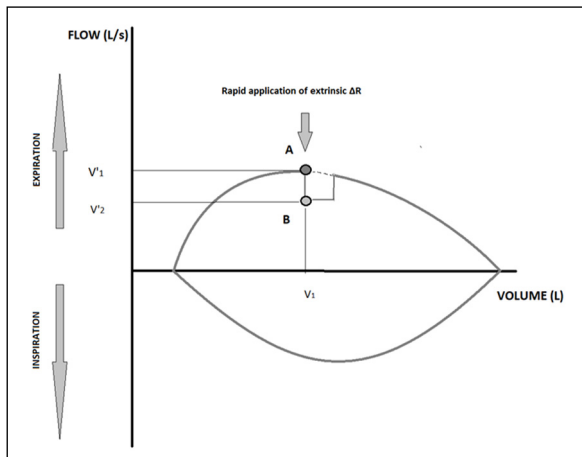


Figure 2. Theoretical flow-volume curve during application of rapid extrinsic resistance (ΔR) during expiration. Expected flow drop ($V'1$ to $V'2$) in an iso-volumic point ($V1$).

not change its driving pressure; thus, the P_{drive} remains virtually unaltered¹⁰. Changes in expiratory or inspiratory volume between the two instances can also be negligible.

By applying equation (1) in those two separate time points, given the P_{drive} , $V(t)$ and compliance (C) remain constant, we can solve it with the only unknown independent variable being the total respiratory resistance (R_{tot}).

$$R_{tot} = V'(t_2) \Delta R / [V'(t_1) - V'(t_2)] \quad \text{Eq. (9)}$$

Where R_{tot} : Total respiratory resistance, ΔR : The stable extrinsic resistance applied, $V'(t_1)$:

flow measured just before the application of ΔR and $V'(t_2)$: flow measured immediately post ΔR application (Figure 2).

It should be noted that R_{tot} is the sum of all respiratory resistances, including airway resistance (R_{aw}), lung tissue resistance (R_l), and chest wall tissue resistance (R_{cw}), regardless of their relative configuration (series/parallel).

Equation (9) can be applied during inspiration or expiration, and hence when R_{tot} is measured in either phase of the respiratory cycle, it reflects the coefficient of the thermal energy loss due to the resistive properties of the moving parts. R_{tot} is subsequently marked as R_{ex} if measured during expiration and R_{in} if measured during inspiration.

Study Design

Development and Connection of Apparatus in the Real-Life Setting

To generate and apply a rapid extrinsic ΔR , we developed new hardware connected in series after the subject and the flow sensor. The configuration used for measuring total respiratory resistance by applying the above theoretical model in a real-life setting is shown in Figure 3 and consists of two separate apparatuses.

The first is a Y-shaped connector tube used to divert flow from the subject and add the aforementioned external resistance (Figure 4). By occluding one branch of the Y apparatus (Point B in Figure 4) with a remote electrical activator, airflow is redirected to the other branch (point

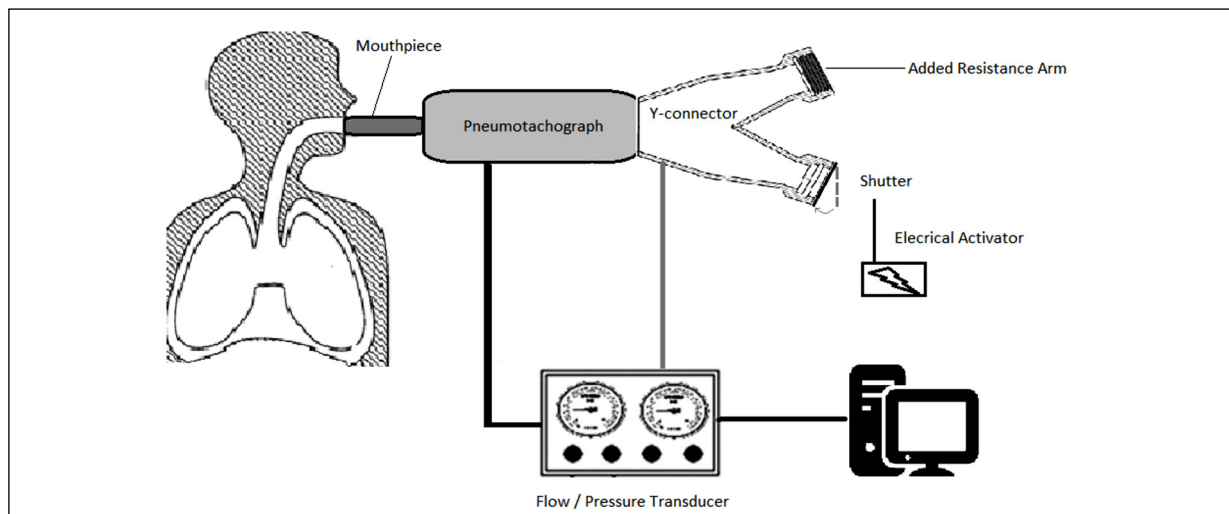
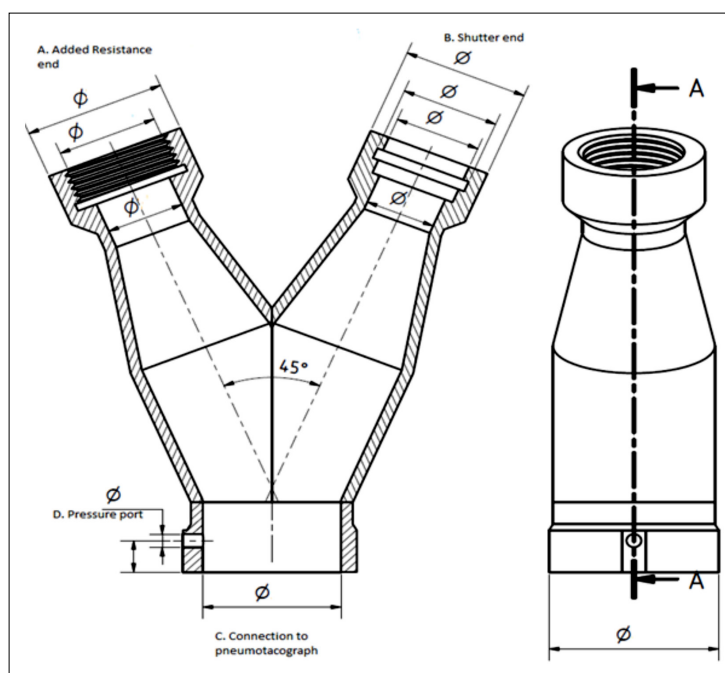


Figure 3. Study model setup.

Figure 4. Schematics of customized mechanical extension connected to the plethysmographs' flow sensor. **A**, Added resistance arm where multiple fine mesh sheets can be applied. **B**, Open-end arm where a rapid electrically operated shutter can be attached. When the shutter is activated, flow is diverted to the added resistance arm (A). **C**, Connection to flow sensor and subject



A), where a steady known resistance is fixed. The back-pressure generated in the area of partial occlusion results in a sudden drop of the flow and a spike rise in the pressure signal recorded by the transducer.

The main stem of the Y-connector is stabilized at the open end of the pneumotachograph. The tube volume (considered an added dead space) was measured at 95 ml, and the radius of the main tube was 1.4 cm while the radius of the branches was 0.7 cm. The length of the arms and central stem and the bifurcation angle of the Y apparatus were minimized (split angle 45°) to keep Reynolds number to a minimum and maintain as laminar flow as possible. A lateral port was used at the wall of the main stem to obtain pressure readings. Thin (1 mm) metal disk-shaped mesh sheets acted as the added resistance and could be stabilized in the open branch of the Y-connector via a screwed mesh holder. The mesh sheets' radius and thickness measured 0.6 cm and 1 mm, respectively.

The second apparatus is the shutter. It consists of an electrically activated moving metal part occluding the tube's opening. The investigator, with a button, manually operates the shutter. The time lag between the manual activation and the airway occlusion is negligible, and the occlusion duration was automatically set to 100ms. Continuous recording of flow and mouth pressure was performed.

Equipment, Procedure and Recordings

All measurements took place at the George D. Behrakis Research Lab[®], Hellenic Cancer Society (Athens, Greece).

Spirometry and body box plethysmography measurements were performed by a specialist technician using a MedGraphics[®] Elite Series[™] Plethysmograph system according to the ERS/ATS task force standards¹¹. The equipment was calibrated as per the manufacturer's guidelines.

The resistance of the respiratory system was evaluated in two separate sessions through two methods. First, body plethysmography (Pleth) was used to measure total, and specific airway resistance (Raw/sRaw)¹². Consequently, we applied the novel method to measure total respiratory resistance during inspiration (Rin) and expiration (Rex).

The subjects were allowed to breathe normally in an upright sitting position until the software automatically scored the FRC line, and three identical breaths in tidal volume were obtained¹³. Then the shutter was activated during multiple breaths, whether in the inspiratory or expiratory phase. The investigators monitored the flow-time and flow-volume loops. During the partial instantaneous occlusion, there was a distinct momentary drop of flow in accord with the increase of mouth pressure and a rapid 'rebound' afterwards to the normal flow when the added resistance was removed. This produced a distinctive 'denting' in the flow-time curve as depicted in Figure 5.

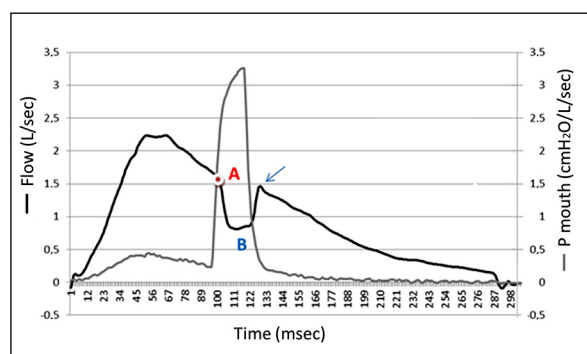


Figure 5. The actual recording of the subject. Flow–Time curve and Mouth Pressure curve during quiet expiration. Point A: Flow before the partial occlusion where $P(t) = VC + V'(t)R_{tot}$. Point B: Flow ‘dent’ when $P_m = \text{peak}$ and $P(t) = VC + V'(t)(\Delta R + R_{tot})$. Arrow: Rebound Flow.

When this ‘dent’ was identified, we established two points in the curve: the first located just before the drop of flow (point A) and the other when P_m reached its peak value (point B). By applying equation (9), and given that $P_{driving}$ remains steady, we could calculate R_{tot} .

ΔR represents the fixed extrinsic resistance generated by the sheets of fine mesh. Each time ΔR was calculated by the difference of P_{mouth} peak (P_{mouth}) and atmospheric pressure (P_{atm} , considered 0) divided by the flow plateau after the occlusion, represented by point B.

$$\Delta R = (P_{mouth} - P_{atm}) / V'(t_B) \quad \text{Eq. (10)}$$

Where t_B is time point B shown in Figure 5.

Since the partial occlusion was performed at the same phase of expiration or inspiration and the flow variability was minimal (between 1 and 1.5 L/sec), air turbulence and added dead space were considered constant.

Data Analysis

Raw digital data of flow, mouth pressure and volume signals were directly obtained from the MedGraphics® Elite Series™ Plethysmograph system software. The time interval between each digitized point measurement of each signal was 0.56 m/s. Using Matlab R2010, LabView®, the signal was processed through a low frequency-pass filter to eliminate background noise and heartbeat oscillations. Continuous waveforms of flow and mouth pressure were synchronized and plotted.

Participants

Fifteen non-ambulatory subjects were enrolled (7 males, mean age 70 ± 15) and assigned to three groups according to their spirometry pattern.

Five individuals (2 males, mean age 67 ± 9) who showed FEV_1 and FVC parameters $>85\%$ of predicted values and normal FEV_1/FVC ratio were assigned to the healthy group. All healthy group subjects were non-smokers with no respiratory disease history and no apparent radiographic abnormalities in the chest X-Ray.

Five individuals (3 males, mean age 65 ± 9) with an obstructive flow-volume curve pattern and FEV_1/FVC ratio $<70\%$ were enlisted in the obstructive group¹⁴. This group included a male ex-smoker, clinically diagnosed with asthma with fixed obstruction, and four individuals with chronic obstructive pulmonary disease (COPD) based on the Global Initiative for Obstructive Lung Disease (GOLD) criteria¹⁵ and compatible radiological abnormalities in previous CT scans¹⁶. According to the GOLD criteria, COPD severity was stage 1 (mild) for one subject, stage 2 (moderate) for two, and stage 3 for two, with a mean FEV_1/FVC ratio of 59%. CT scans of obstructive patients with COPD revealed mainly emphysematous abnormalities of various severity with or without coexisting bronchiectasis but no indication of concurrent interstitial disease.

Five patients (2 males, mean age 77 ± 9) were enrolled in the restrictive group; four presented with idiopathic pulmonary fibrosis (IPF) and one with obesity hypoventilation syndrome diagnosis. IPF was diagnosed according to the ATS/ERS classification criteria¹⁷, and all patients had CT scans with compatible abnormalities¹⁸. Spirometry and flow-volume loop showed a restrictive pattern with FEV_1/FVC ratio $>85\%$ and FVC $<70\%$.

Participants were informed of the study’s scope and their right to access and withdraw at any time. Each participant gave his/her written informed consent before beginning the study. Ethics approval was granted from the Ethics Committee of the School of Medicine, National Kapodistrian University of Athens.

Validation of Method

The repeatability of R_{tot} measurements was validated with three approaches. First, multiple partial occlusions were performed during quiet breathing in at least six respiratory cycles (three inspiratory and three expiratory) and mean R_{tot}

was calculated in each one. Second, an increasing number of fine mesh sheets were added, and the procedure was repeated each time the applied ΔR changed. The minimum number of fine mesh sheets that needed to be applied to detect a flow ‘denting’ was 7, generating a mean resistance of 1.2 cm H₂O/L/sec using Eq. (10). Two more measurements were then obtained with a 2-fold and 3-fold increase of the added resistance (i.e. 14 and 21 mesh sheets producing 1.9 and 2.5 cm H₂O/L/sec respectively). If more sheets were added, the subject was able to perceive the occlusion.

Finally, using R_{tot} as a known variable, equation (9) was solved with the unknown variable being the ΔR (ΔR_1) and was then compared with the actual measured extrinsic resistance (ΔR_2).

Figure 6 shows three different ΔR_1 vs. ΔR_2 coefficient plots for three subjects- one from each group- using the computed R_{tot} as a fixed variable and changing the value of added resistance.

Statistical Analysis

Comparison between R_{aw} , R_{in} and R_{ex} among groups was performed using Welch paired t-test. Statistical significance between R measured and

R Validated was performed for each added resistance increment using paired t-test. Linear regression analysis was performed between R_{in} and R_{ex} with R_{aw} and sR_{aw} parameters obtained from the plethysmography.

Results

Fifteen subjects were investigated: five healthy, five with obstructive and five with restrictive spirometry patterns. Table I summarizes the subjects’ characteristics and measurements. The restrictive group showed the lowest FVC, and the obstructive group had the lowest FEV₁. The highest R_{aw} and sR_{aw} were noted in the obstructive group at 5.01 (± 1.04) cm H₂O/L/sec and 18.66 (± 2.65) cm H₂O/L/sec/L, respectively.

The mean R_{in} in the healthy group was 4.99 cm H₂O/L/sec, and the mean R_{ex} was 4.42 cm H₂O/L/sec. The obstructive group exhibited a mean R_{in} of 4.87 cm H₂O/L/sec and a mean R_{ex} of 6.63 cm H₂O/L/sec. In the restrictive group, mean R_{in} was 5.97 cm H₂O/L/sec, and mean R_{ex} was 4.12 cm H₂O/L/sec. R_{ex} was notably higher than R_{in} exclusively in the obstructive

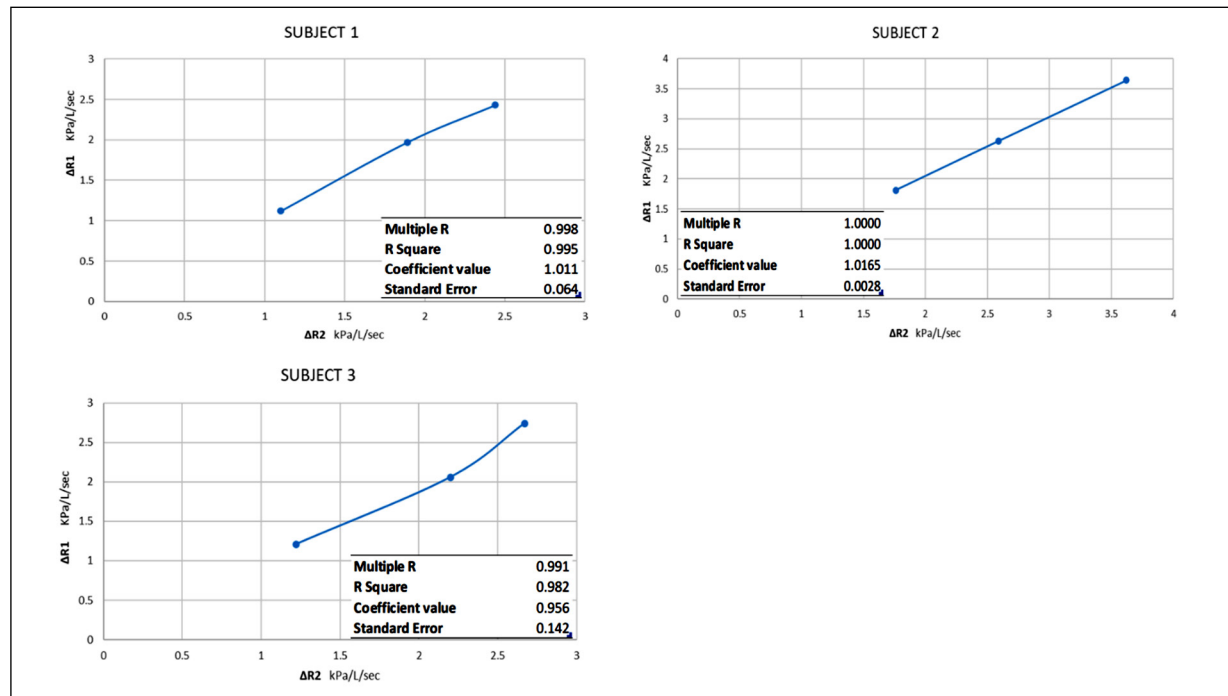


Figure 6. ΔR Validation. Within each subject, we compared the measured ΔR (ΔR Measured) with the predicted ΔR (ΔR Validated) if R_{tot} was fixed and Eq.(2) was solved, considering ΔR the unknown variable. No statistical significance was noted between ΔR Measured (ΔR_1) and ΔR Validated (ΔR_2) in all patients and with the increase in the number of fine mesh sheets. Mean ΔR (both measured and validated) showed a homogenous decline with the rise of fine mesh sheets.

Table I. Participants' characteristics and Spirometry/Plethysmography results.

Groups	Healthy	Obstructive	Restrictive
N	5	5	5
Age	67 (+/- 9)	65 (+/- 6)	77 (+/- 9)
Sex (male/female)	2/3	3/2	2/3
BMI (Kg/m ²)	26 (+/- 6)	25 (+/- 2)	28 (+/- 15)
Smoking (Current/ex/never)	0/0/0	4/1/0	1/2/2
Diagnosis		4: COPD, 1: Asthma	4: IPF, 1: OHS
FEV ₁ (% predicted)	101 (+/- 2)	62 (+/- 2)	79 (+/- 6)
FVC (% predicted)	102 (+/- 3)	82 (+/- 6)	65 (+/- 2)
FEV ₁ /FVC	75 (+/- 1)	61 (+/- 3)	86 (+/- 2)
SVC (% predicted)	97 (+/- 3)	89 (+/- 2)	67 (+/- 3)
TLC (% predicted)	98 (+/- 4)	92 (+/- 4)	60 (+/- 5)
FRC (% predicted)	100 (+/- 2)	110 (+/- 2)	63 (+/- 3)
RV (% predicted)	86 (+/- 4)	107 (+/- 3)	56 (+/- 5)
Raw (cm H ₂ O/L/sec)	2.77 (+/- 0.023)	5.01 (+/- 0.102)	2.59 (+/- 0.067)
sRaw (cm H ₂ O /L/sec/L)	6.83 (+/- 0.13)	18.66 (+/- 0.26)	6.22 (+/- 0.19)

BMI: body mass index, FEV₁: forced expiratory volume in 1s, FVC: forced vital capacity, SVC: slow vital capacity, TLC: total lung capacity, FRC: functional residual capacity, RV: residual volume, Raw: airway resistance, sRaw: specific airway resistance, COPD: chronic obstructive lung disease, IPF: idiopathic pulmonary fibrosis, OHS: obesity hypoventilation syndrome.

group ($p < 0.001$). Rin was significantly higher in the restrictive group compared to the healthy and obstructive group ($p < 0.001$) (Figure 7).

Rex was positively correlated with Raw and sRaw in the obstructive group with a p -value of 0.0235 and $r = 0.47$. Although no statistical significance was proved ($p > 0.05$), Rin was positively correlated with sRaw within the restrictive group.

The mean absolute difference between expiratory and inspiratory resistance ($\delta Rrs = |Rex| - |Rin|$) was 0.6 cm H₂O/L/sec in the control group, 0.9 cm H₂O/L/sec and 1.6 cm H₂O/L/sec in the obstructive and restrictive group, respectively. Although Rin was higher than Rex in the control and the restrictive subgroup of subjects, δRrs was significantly higher in the latter ($p < 0.001$).

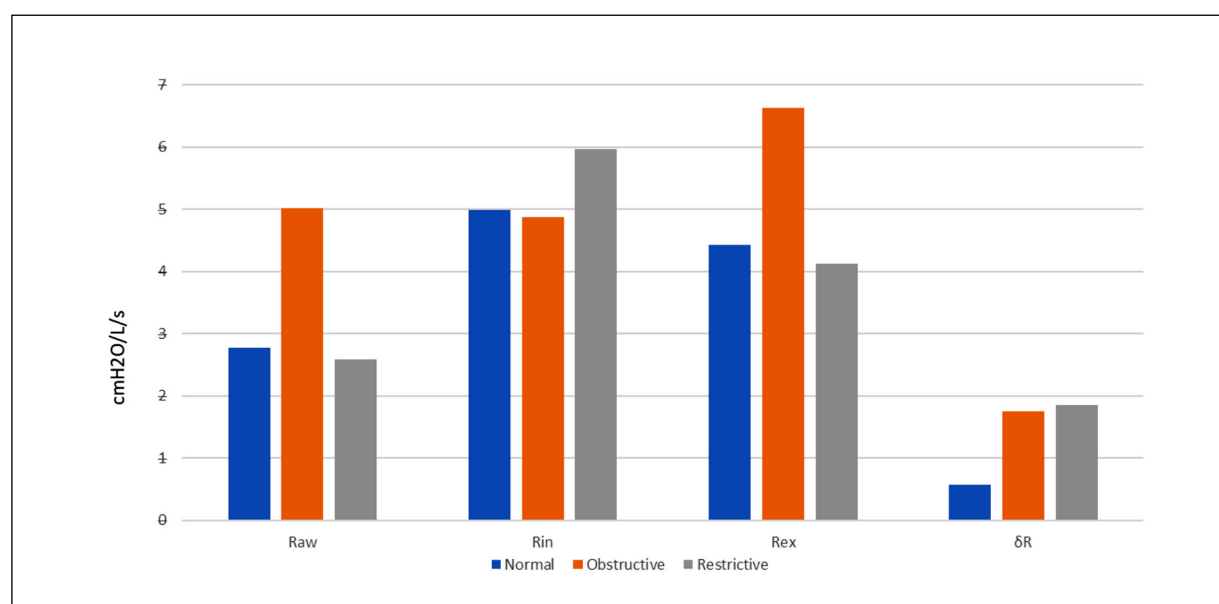


Figure 7. Comparison between Raw, Rin, Rex and absolute difference of the two (δRrs) in the three subject groups (Healthy, Obstructive, Restrictive). Raw: Airway respiratory resistance, Rin: inspiratory resistance, Rex: expiratory resistance, δRrs : the absolute difference between inspiratory and expiratory resistance.

Validation analysis did not show a significant statistical difference between $\Delta R1$ and $\Delta R2$ in 3 randomly selected patients from all groups in three separate measurements with increasing external added resistance.

A comparison of $\Delta R1$ (measured) vs. $\Delta R2$ (validated) revealed no significant difference for all pairs of values within each resistance increment ($r=1, p=0.786$).

Discussion

The current study is the first to present a novel method for respiratory mechanics evaluation during resting breathing.

We developed a mathematical model applied in a real-life setting during tidal breathing. Total respiratory resistance was measured, requiring minimal patient cooperation, while our results were validated with acceptable repeatability in healthy and individuals with respiratory disorders.

The new method succeeded in capturing distinct alterations of the inspiratory and expiratory components of resistance that allow the differentiation between an obstructive and restrictive pattern of impairment. Furthermore, as it only requires resting breathing, it offers an easy alternative for total resistance measurement, especially for patients unable to undergo the forced manoeuvres of routine pulmonary function testing.

Three different resistance response patterns were observed, corresponding to the healthy, obstructive and restrictive groups. In healthy subjects, the total respiratory resistance, including airways, lung tissue and chest wall, was slightly increased during inspiration. The opposite effect was noted in patients with obstructive diseases such as asthma or COPD, where the expiratory R_{tot} was elevated. This can be logically attributed to the increased resistance of narrowed airways in these patients (i.e. increased R_{aw})¹⁹. In contrast, patients with restrictive diseases such as interstitial lung disease or obesity hypoventilation syndrome displayed an increased inspiratory R_{tot} that can be attributed to the increased lung tissue (RL) or chest wall (R_{cw}) resistive properties, respectively.

R_{tot} is the sum of the resistive elements that govern all the respiratory system's moving parts (i.e. column of air in the airways, lung parenchyma, chest wall etc.). Since the novel method requires only a partial instantaneous interruption

of flow, and the glottis remains open, the pressure measured at the mouthpiece reflects both the elastic recoil pressure (P_{el}) and the resistive flow pressure of the airways (P_{aw}).

Our results are in coherence with the findings of previous studies reflecting the main pathophysiological changes in obstructive and restrictive disorders^{20,21}. As expected, obstructive patients present an increase of R_{ex} , mainly reflecting the increase in airways' expiratory flow resistive pressure (R_{aw})²². R_{ex} and R_{aw} of the obstructive group were positively correlated in our analysis.

Restrictive patients exhibited increased R_{in} , which mirrors the potential increase in lung parenchyma's elastic recoil pressure. However, such measurement is not routinely performed and requires special invasive instruments and setting to determine transpulmonary pressure and lung compliance (i.e., oesophageal balloon catheter). Thus, there is no available comparative index to correlate with R_{in} measurements.

Our study has several limitations, including a limited number of subjects and observations. However, this study was not designed as a prospective one and aimed mainly to describe the methodology and investigate feasibility. The technical apparatus applied was developed and realized by our team and has not been standardized yet.

Conclusions

This technique can be used in other settings, albeit we recognize that this might be challenging. Future studies might provide more extensive evidence of this method's clinical value and compare it with other modalities such as impulse oscillometry systems.

Conflict of Interest

The Authors declare that they have no conflict of interests.

Acknowledgements

Anagnostopoulos Nektarios, Tzortzi Anna, Evangelopoulou Vasiliki, Behrakis Panagiotis: Conceptualization, Methodology, Software. Anagnostopoulos Nektarios, Kaltsakas Georgios: Data Curation. Anagnostopoulos Nektarios, Tzortzi Anna, Cholidou Kyriaki, Koukaki Evangelia, Kaltsakas Georgios: Writing, Original draft preparation, Visualization, Investigation. Behrakis Panagiotis, Stratakos Grigorios, Koutsilieris Michael: Supervision.

Funding

No funding was received.

Informed Consent

Informed consent was obtained from all participants.

References

- 1) Cheung HJ, Cheung L. Coaching patients during pulmonary function testing: A practical guide. *Can J Respir Ther* 2015; 51: 65-68.
- 2) Miller MR, Hankinson J, Brusasco V, Burgos F, Casaburi R, Coates A, Crapo R, Enright P, Van der Grinten CPM, Gustafsson P, Jensen R, Johnson DC, MacIntyre N, McKay R, Navajas D, Pedersen OF, Pellegrino R, Viegi G, Wagner J, ATS/ERS Task Force. Standardization of spirometry. *Eur Respir J* 2005; 26: 319-338.
- 3) De Mir Messa I, Sardón Prado O, Larramona H, Salcedo Posadas A, Villa Asensi JR. Body plethysmography (i): Standardisation and quality criteria. *An Pediatría* 2015; 83: 136.
- 4) Gappa M, Colin AA, Goetz I, Stocks J. Passive respiratory mechanics: the occlusion techniques. *Eur Respir J* 2001; 17: 141-148.
- 5) Bickel S, Popler J, Lesnick B, Eid N. Impulse oscillometry: Interpretation and practical applications. *Chest* 2014; 146: 841-847.
- 6) Smith HJ, Reinhold P, Goldman MD. Forced oscillation technique and impulse oscillometry. *Eur Respir Mon* 2005; 31: 72-105.
- 7) Apostólico N, Urbano JJ, Kelly da Palma R, Vieira RDP, Brandao GS, Uriarte JJ, Oliveira LVF. Mathematical models for measuring mechanical properties in experimental animal lung: A literature review. *Med Sci Tech* 2015; 56: 1-9.
- 8) Ghafarian P, Jamaati H, Hashemian SM. A review on human respiratory modeling. *Tanaffos* 2016; 15: 61-69.
- 9) Otis AB, Mckerrow CB, Bartlett RA, Mead J, McIlroy MB, Selver-Stone NJ, Radford Jr EP. Mechanical factors in distribution of pulmonary ventilation. *J Appl Physiol* 1956; 8: 427-443.
- 10) Bates JHT, Rossi A, Milic-Emili J. Analysis of the behavior of the respiratory system with constant inspiratory flow. *J Appl Physiol* 1985; 58: 1840-1848.
- 11) Graham BL, Steenbruggen I, Miller MR, Barjaktarevic IZ, Cooper BG, Hall GL, Hallstrand TS, Kaminsky DA, McCarthy K, McCormack MC, Oropoz CE, Rosenfeld M, Stanojevic S, Swanney MP, Thompson BR. Standardization of Spirometry 2019 Update. An Official American Thoracic Society and European Respiratory Society Technical Statement. *Am J Respir Crit Care Med* 2019; 200: 70-88.
- 12) Stocks J, Godfrey S, Beardsmore C, Bar-Yishay E, Castile R. Plethysmographic measurements of lung volume and airway resistance. *Eur Respir J* 2001; 17: 125.
- 13) Kuhlen R, Mohnhaupt R, Slama K, Hausmann S, Pappert D, Rossaint R, Falke K. Validation and clinical application of a continuous P0.1 measurement using standard respiratory equipment. *Technol Health Care* 1996; 4: 415-424.
- 14) Miller MR, Steenbruggen I, Quanjer PH, Ruppel G, Crapo RO, Pedersen OF. Defining the lower limit of normal for FEV₁/FVC. *Am J Respir Crit Care Med* 2007; 176: 101.
- 15) Rabe KF, Hurd S, Anzueto A, Barnes PJ, Buist SA, Calverley P, Fukuchi Y, Jenkins C, Rodriguez-Roisin R, Weel CV, Zielinski J. Global Strategy for the Diagnosis, Management, and Prevention of Chronic Obstructive Pulmonary Disease GOLD Executive Summary *Am J Respir Crit Care Med* 2013; 187: 347-365.
- 16) O'Brien C, Guest PJ, Hill SL, Stockley RA. Physiological and radiological characterization of patients diagnosed with chronic obstructive pulmonary disease in primary care. *Thorax* 2000; 55: 635-642.
- 17) Raghu G, Remy-Jardin M, Myers JL, Richeldi L, Ryerson CJ, Lederer DJ, Behr J, Cottin, Danoff SK, Morell F, Flaherty KR, Wells A, Martinez FJ, Azuma A, Bice TJ, Bouros D, Brown KK, Collard HR, Duggal A, Galvin L, Inoue Y, Jenkins RG, Johkoh T, Kazerooni EA, Kitaichi M, Knight SL, Mansour G, Nicholson AG, Pipavath SNJ, Bueñía-Roldán I, Selman M, Travis WD, Walsh SLF, Wilson KC. Diagnosis of idiopathic pulmonary fibrosis An Official ATS/ERS/JRS/ALAT Clinical practice guideline. *Am J Respir Crit Care Med* 2018; 198: 44-68.
- 18) Souza CA, Müller NL, Flint J, Wright JL, Churg A. Idiopathic Pulmonary Fibrosis: Spectrum of High-Resolution CT Findings. *Am J Roentgenol* 2005; 185: 1531-1539.
- 19) Kaminsky DA. What does airway resistance tell us about lung function? *Respir Care* 2012; 57: 85-99.
- 20) Shirai T, Kurosawa H. Clinical application of the forced oscillation technique. *Intern Med* 2016; 55: 559-566.
- 21) Sue DY. Measurement of lung volumes in patients with obstructive lung disease. *Ann Am Thorac Soc* 2013; 10: 525-530.
- 22) Sugiyama A, Hattori N, Haruta Y, Nakamura I, Nakagawa M, Miyamoto S, Onari Y, Iwamoto H, Ishikawa N, Fujitaka K, Murai H, Kohno N. Characteristics of inspiratory and expiratory reactance in interstitial lung disease. *Respir Med* 2013; 107: 875-882.